Supplementary Information

High-entropy Engineering Tuning Electrochemical Activity and Stability of Layered Double Perovskite Oxygen Electrode for High-Performance Protonic Ceramic Cells

Zhipeng Sun[a], Zhihong Du[a,b], Konrad Świerczek[c], Jianrong Zeng[d,e], Hailei Zhao[a,b,*]

[a] *School of Materials Science and Engineering, University of Science and Technology Beijing, Beijing 100083, P.R. China*

[b] *Beijing Municipal Key Lab for Advanced Energy Materials and Technologies, Beijing 100083, PR China*

[c] *Faculty of Energy and Fuels, AGH University of Krakow, al. A. Mickiewicza 30, Krakow, 30-059, Poland*

[d] *Shanghai Synchrotron Radiation Facility, Shanghai Advanced Research Institute, Chinese Academy of Sciences, Shanghai 201204, P.R. China.*

[e] *Shanghai Institute of Applied Physics, Chinese Academy of Sciences, Shanghai 201800, P. R. China.*

[*]hlzhao@ustb.edu.cn

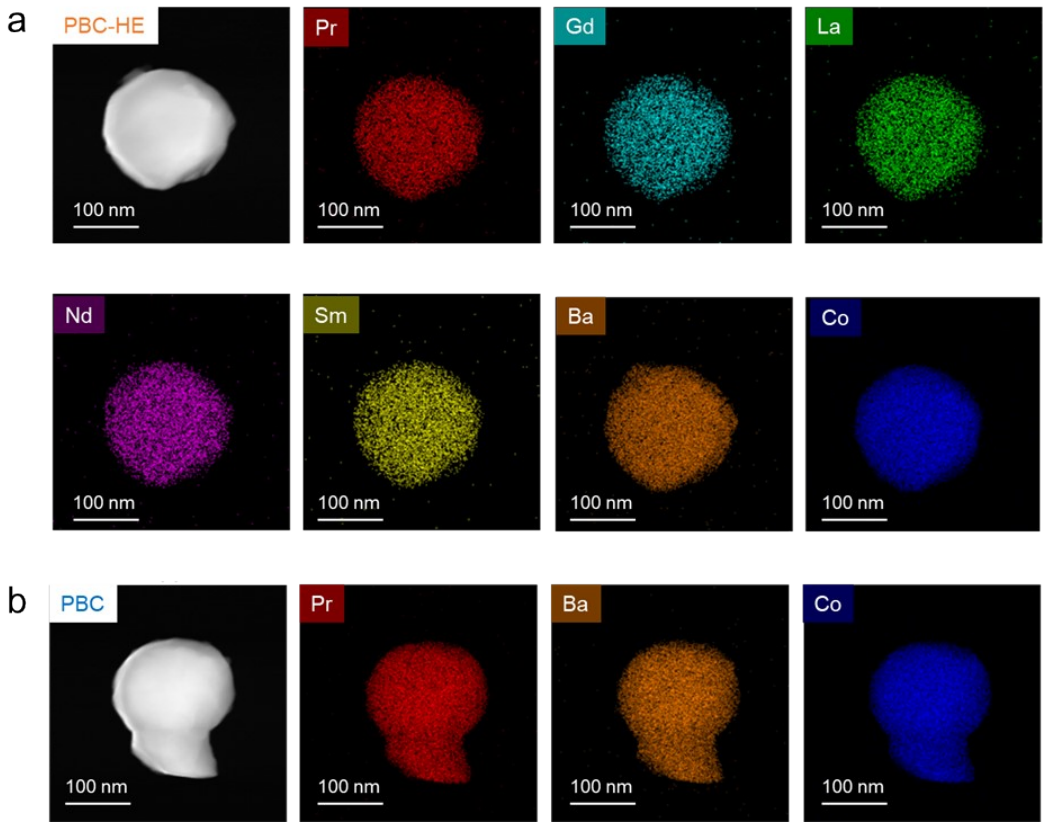

Figure S1. HAADF-STEM image and EDX elemental mapping of Pr, La, Sm, Nd, Gd, Ba and Co for PBC-HE (a) and PBC (b).

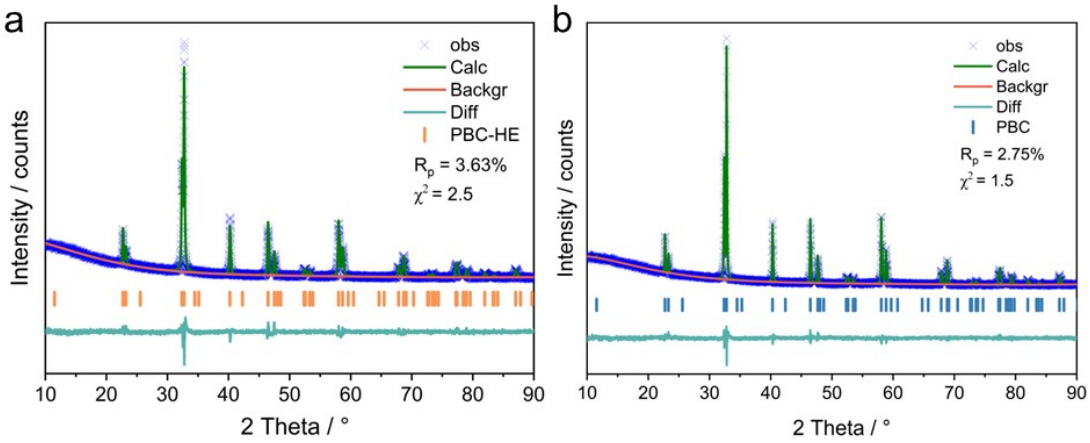

Figure S2. XRD patterns with Rietveld refinement of samples PBC-HE (a) and PBC (b). Both fittings were performed with tetragonal *P*4/*mmm* space group.

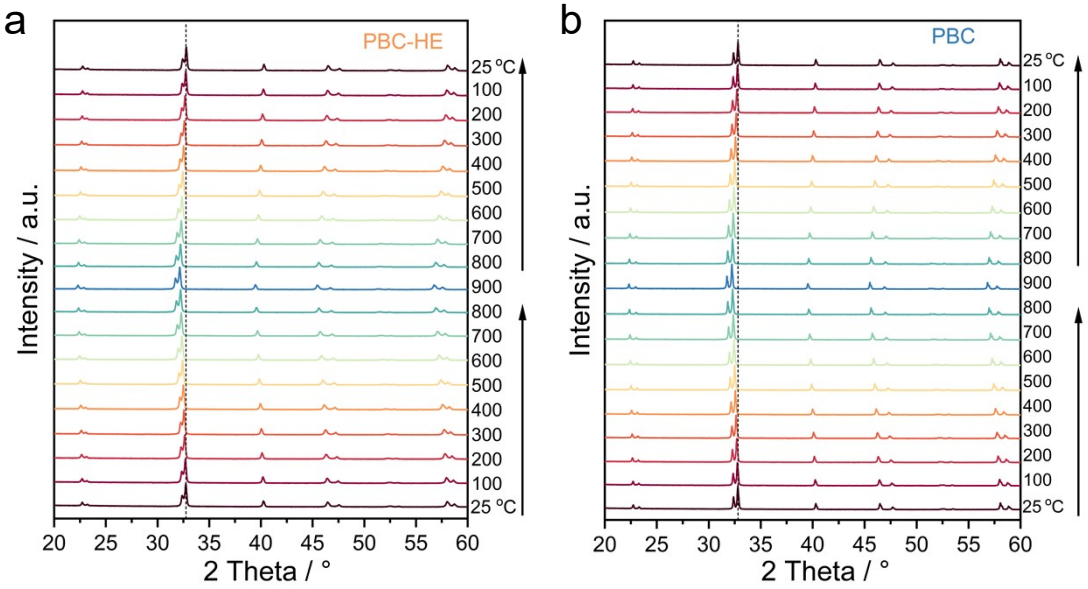

Figure S3. High temperature XRD patterns of PBC-HE (a) and PBC (b) obtained in temperature range of 25-900 °C

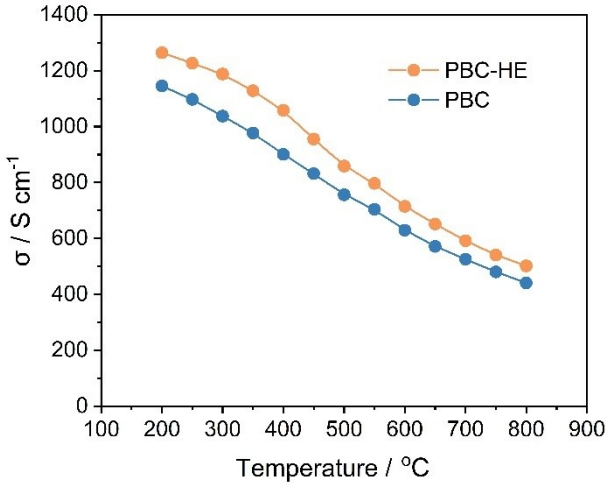

Figure S4. Electrical conductivity of samples PBC-HE and PBC as a function of temperature in air.

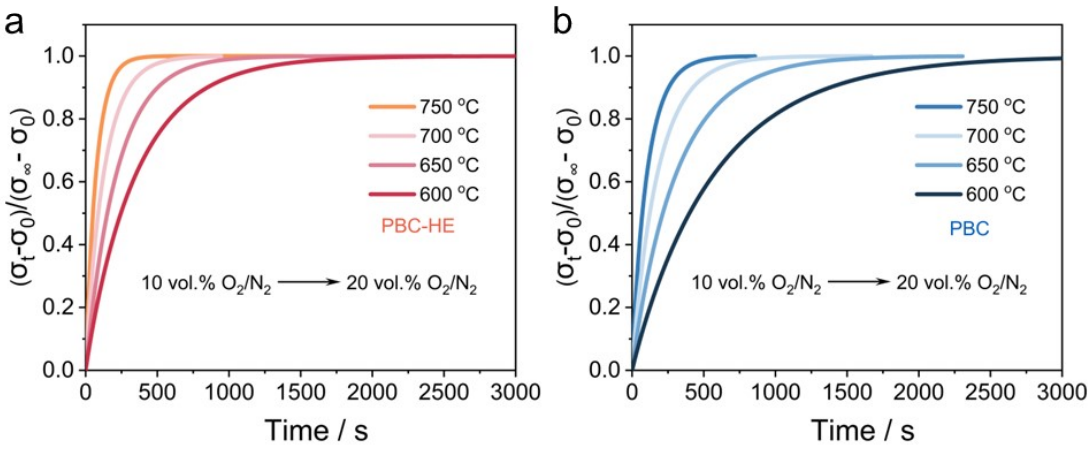

Figure S5. Normalized relationship between conductivity and testing time of samples PBC-HE (a) and PBC (b), after fast switching the ambient gas from 10 vol.% to 20 vol.% O_2/N_2. Data recorded in temperature range of 600-750 °C.

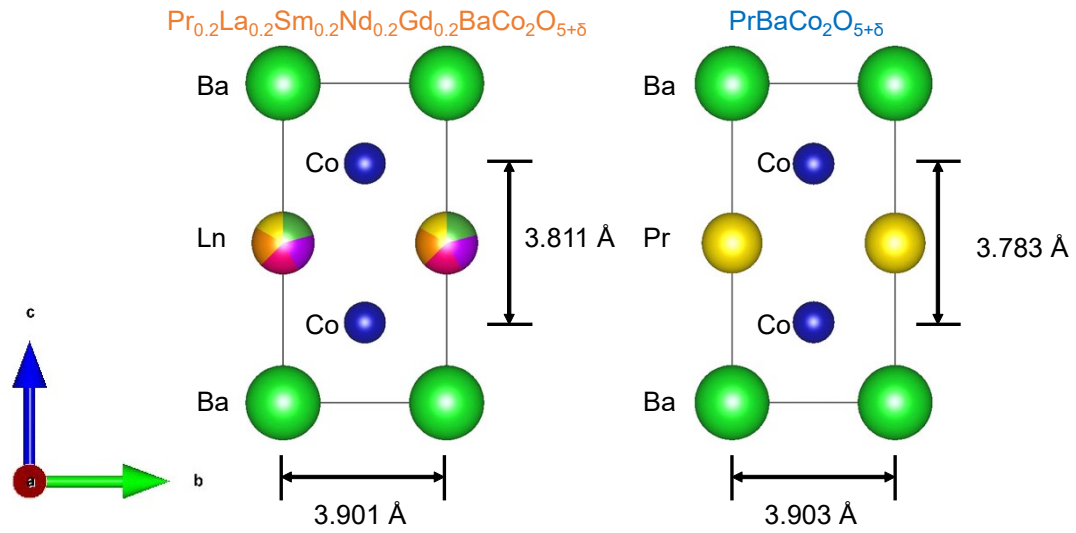

Figure S6. Rare-earth metal layer spacing of samples PBC-HE and PBC derived from XRD Rietveld refinement at room temperature.

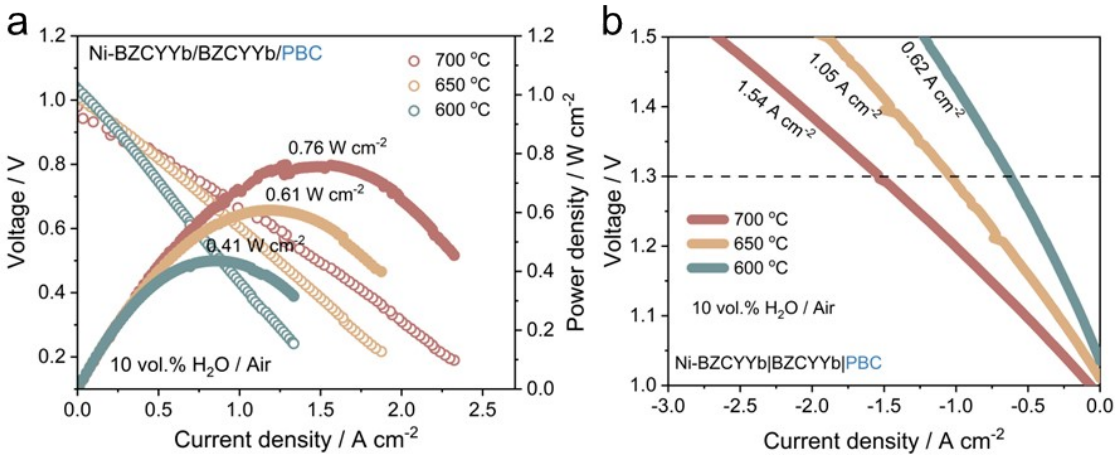

Figure S7. *I-V* and *I-P* curves in fuel cell mode (a) and *I-V* curves in electrolysis mode (b) with 10 vol.% H_2O in air provided to oxygen electrode, for the full cell with Ni-BZCYYb|BZCYYb|PBC configuration.

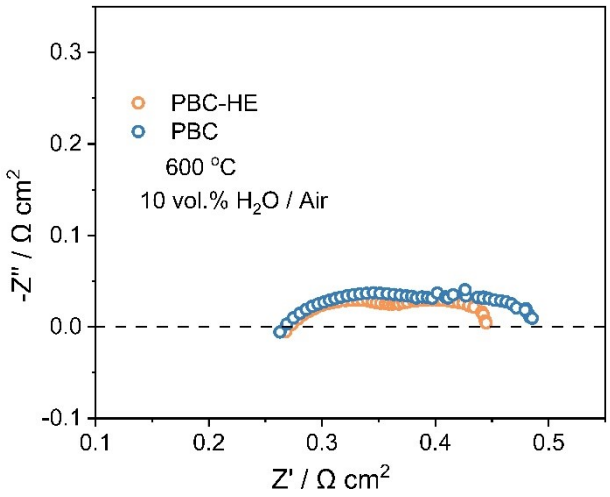

Figure S8. Comparison of electrochemical impedance spectra of full cells with PBC-HE and PBC as oxygen electrodes, respectively. The data were recorded at 600 ℃ with 10 vol.% H_2O/air provided to the oxygen electrodes.

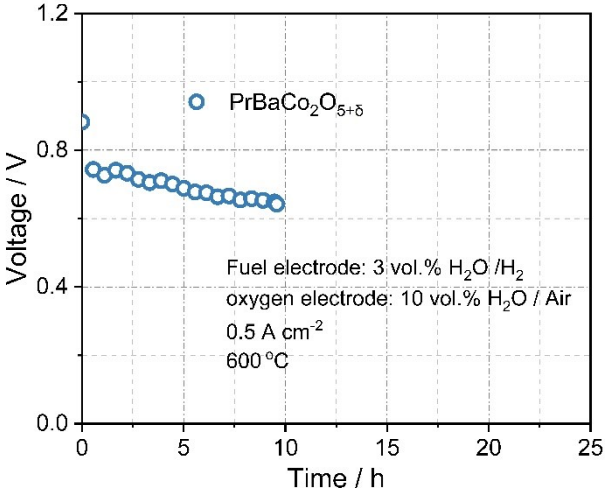

Figure S9. Short-term stability of Ni-BZCYYb|BZCYYb|PBC full cell with PBC as oxygen electrode in fuel cell mode.

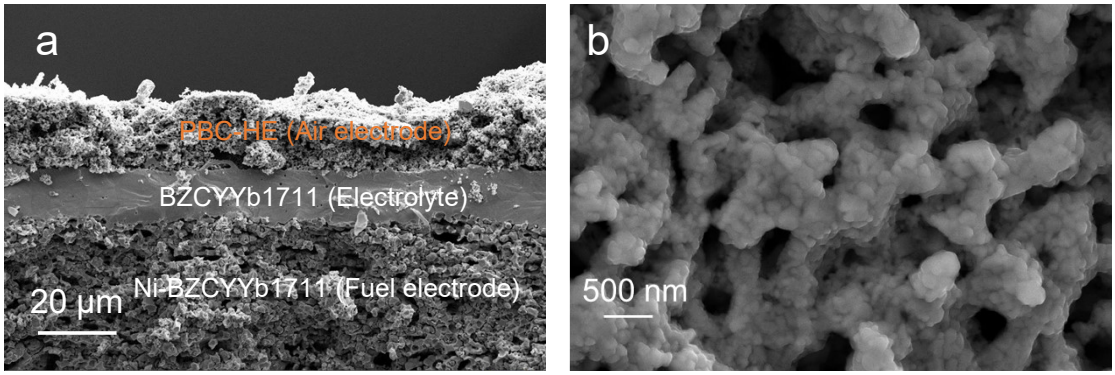

Figure S10. Cross-section micrograph of the Ni-BZCYYb|BZCYYb|PBC-HE full-cell after FC/EC mode alternative operation (a). Surface morphology of PBC-HE oxygen electrode after fuel cell/electrolysis mode cycling tests for 90 h (b).

Note S1

The Co $2p_{3/2}$ of PBC-HE and PBC samples before and after long-term stability test are shown in Figure S11. For the as-prepared PBC-HE and PBC samples (Figure S11a), the binding energy at 781 eV are assigned to Co^{4+}, while those at 778.5 eV correspond to Co^{3+}, respectively[1]. The average valence state of Co ions in PBC-HE is calculated to be 3.34, which is lower than that in PBC (3.39), indicating a higher concentration of oxygen vacancies in PBC-HE, which is consistent with the TG results (Figure 1d). After the long-term operation in vapor atmosphere, the average oxidation states of Co in both

PBC-HE and PBC increased to 3.48 and 3.43, respectively (Figure S11b), suggesting a decrease in oxygen vacancy concentration. This change can be attributed to the adsorption of water molecules (protonation process), which cause the occupying of oxygen vacancy by oxygen from water and the generation of protons (Equation 2). It is worth noting that the PBC-HE exhibits a more pronounced increase in the Co oxidation state, suggesting its enhanced proton-uptake capability, which is in agreement with the hydration TG results (Figure 3a, b).

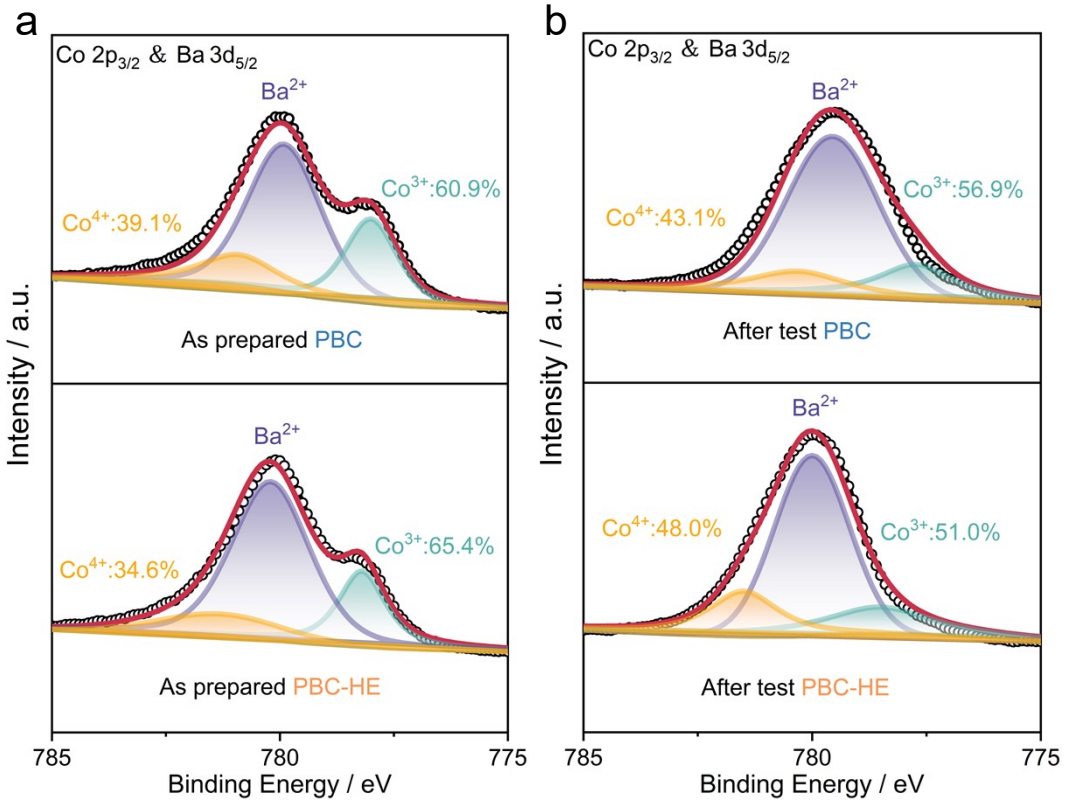

Figure S11. XPS spectra of Co $2p_{3/2}$ of samples PBC-HE and PBC before (a) and after (b) long-term stability test in 10 vol.% H_2O/Air.

Table S1. Refined lattice parameters of samples PBC-HE and PBC at room temperature.

Samples	Space group	*a* (Å)	*c* (Å)	*V* (Å)	χ^2	R_{wp} (%)
PBC-HE	*P*4/*mmm*	3.900(8)	7.643(1)	116.32(8)	2.5	3.63
PBC	*P*4/*mmm*	3.903(4)	7.613(0)	115.88(1)	1.5	2.75

Table S2. Oxygen content ($5+\delta$) and average valence state of cobalt of samples PBC-HE and PBC at room temperature.

Sample	$5+\delta$	n
PBC-HE	5.698	3.198
PBC	5.773	3.273

Table S3. Refined lattice parameters of PBC-HE and PBC samples, obtained in the temperature range of 25-900 ℃ on heating and cooling.

	PBC-HE			PBC		
T / ℃	a / Å	c / Å	R_{wp} (%)	a / Å	c / Å	R_{wp} / %
25	3.901(1)	7.643(4)	3.58	3.903(3)	7.613(0)	2.78
100	3.904(9)	7.657(9)	3.59	3.907(6)	7.626(4)	2.79
200	3.910(8)	7.676(5)	3.68	3.914(1)	7.643(7)	2.78
300	3.917(9)	7.695(0)	3.61	3.921(5)	7.661(1)	2.78
400	3.929(5)	7.708(3)	3.64	3.932(3)	7.674(6)	2.76
500	3.941(3)	7.722(0)	3.52	3.943(2)	7.688(4)	2.88
600	3.953(1)	7.736(2)	3.53	3.953(9)	7.702(4)	2.80
700	3.964(4)	7.750(8)	3.54	3.964(5)	7.717(1)	2.84
800	3.975(9)	7.765(7)	3.51	3.975(1)	7.732(3)	2.81
900	3.987(2)	7.784(2)	3.50	3.985(4)	7.748(3)	2.86
800	3.975(9)	7.765(6)	3.49	3.975(1)	7.732(1)	2.89
700	3.964(5)	7.751(0)	3.43	3.964(6)	7.716(9)	2.81
600	3.953(0)	7.735(5)	3.52	3.954(0)	7.702(5)	2.83
500	3.941(5)	7.722(2)	3.62	3.943(2)	7.688(4)	2.79
400	3.929(8)	7.708(2)	3.61	3.932(2)	7.674(6)	2.79
300	3.918(1)	7.693(0)	3.62	3.921(5)	7.660(5)	2.83

200	3.910(8)	7.675(1)	3.57	3.914(2)	7.643(4)	2.76
100	3.904(9)	7.657(0)	3.66	3.907(6)	7.626(0)	2.76
25	3.900(8)	7.643(4)	3.63	3.903(4)	7.613(1)	2.75

Table S4. Surface oxygen exchange coefficients K_{ex} of samples PBC-HE and PBC at different temperatures.

Temperature / °C	PBC-HE, $K_{ex} \times 10^4$ /cm s^{-1}	PBC, $k_{ex} \times 10^4$ / cm s^{-1}
750	6.16	5.56
700	4.34	3.54
650	2.65	2.01
600	1.55	1.17

Table S5 Electrode reaction kinetics process for $H_2O \leftrightarrow H_2 + 0.5\ O_2$ (g).

Steps	Electrode reactions
1	$H_2O(g) \leftrightarrow H_2O_{ad}$
2	$H_2O_{ad} + 2O_O^{\times} \leftrightarrow 2OH_{O+}^{\cdot} + O_{ad}^{''}$
3	$O_{ad}^{''} - 2e^{'} \leftrightarrow 2O_{ad}$
4	$2O_{ad} \leftrightarrow \frac{1}{2}O_2(g)$
5	$OH_{O,\,electrode}^{\cdot} \leftrightarrow OH_{O,\,electrolyte}^{\cdot}$

Table S6. Performance comparison of the developed PBC-HE, PBC and other reported high-performance oxygen electrodes.

Oxygen electrode	ASR (Ω cm^{-2})[a]	T (^{o}C)	Electrolyte (Thickness in μm)	P_{max} (W cm^{-2})	Current density at 600 °C, 1.3 V, (A cm^{-2})	Ref.
$PrBaCo_{1.5}Fe_{0.5}O_{5+\delta}$	0.125 0.26 0.72	700 650 600	$BaZr_{0.1}Ce_{0.7}Y_{0.1}Yb_{0.1}O_{3-\delta}$ (~50)	0.51 0.40 0.28	-0.5 (30% H_2O)	[2]
$Ba_{0.95}K_{0.05}Co_{0.2}Zn_{0.2}Ga_{0.2}Zr_{0.2}Y_{0.2}O_{3-\delta}$	0.049 0.152 0.354	700 650 600	$BaZr_{0.1}Ce_{0.7}Y_{0.1}Yb_{0.1}O_{3-\delta}$ (~11)	1.33 0.77 0.56	-0.99	[3]
$LaPr_{0.2}Sm_{0.2}Ba_{0.2}Sr_{0.2}Ca_{0.2}NiO_{4+\delta}$	0.036 0.077 0.206	700 650 600	$BaZr_{0.1}Ce_{0.7}Y_{0.1}Yb_{0.1}O_{3-\delta}$ (~7)	2.00 1.57 1.08	-	[4]
$Pr_{0.2}La_{0.2}Nd_{0.2}Na_{0.2}Ca_{0.2}Ba_{0.5}Sr_{0.5}Co_{1.5}Fe_{0.5}O_{5+\delta}$	0.045 0.107 0.301	700 650 600	$BaZr_{0.4}Ce_{0.4}Y_{0.1}Yb_{0.1}O_{3-\delta}$ (~5)	3.01 1.77 1.02	-0.86 (3% H_2O)	[5]
$Pr_{1/6}La_{1/6}Nd_{1/6}Ba_{1/6}Sr_{1/6}Ca_{1/6}CoO_{3-\delta}$	0.06 0.12 0.26	700 650 600	$BaZr_{0.1}Ce_{0.7}Y_{0.1}Yb_{0.1}O_{3-\delta}$ (~10)	- 1.51 1.16	-1.75	[6]
$Pr_{0.2}Ba_{0.2}Sr_{0.2}La_{0.2}Nd_{0.2}CoO_{3-\delta}$	0.19 0.51 1.40	700 650 600	$BaZr_{0.1}Ce_{0.7}Y_{0.1}Yb_{0.1}O_{3-\delta}$ (~6.5)	1.55 0.87 0.42	-0.67 (3% H_2O)	[7]
$La(Co_{0.2}Cu_{0.2}Fe_{0.2}Ni_{0.2}Cr_{0.2})O_{3-\delta}$	- 0.22 0.27	700 650 600	$BaZr_{0.6}Ce_{0.2}Y_{0.1}Yb_{0.1}O_{3-\delta}$ (~14)	- 0.60 0.41	-1.18 (3 % H_2O)	[8]
$Pr_{0.2}La_{0.2}Sm_{0.2}Nd_{0.2}Gd_{0.2}BaCo_2O_{5+\delta}$ (PBC-HE)	0.064 0.148 0.367	700 650 600	$BaZr_{0.1}Ce_{0.7}Y_{0.1}Yb_{0.1}O_{3-\delta}$ (~15)	1.01 0.75 0.51	-0.73 (10% H_2O)	**This work**
$PrBaCo_2O_{5+\delta}$ (PBC)	0.098 0.202 0.434	700 650 600	$BaZr_{0.1}Ce_{0.7}Y_{0.1}Yb_{0.1}O_{3-\delta}$ (~15)	0.76 0.61 0.41	-0.62 (10% H_2O)	**This work**

a) Symmetrical cell

References

1 F. He, F. Zhu, D. Liu, Y. Zhou, K. Sasaki, Y. Choi, M. Liu and Y. Chen, *Mater. Today*, 2023, **63**, 89-98.

2 J Feng, X Feng, C Xie, P Wang, T Cong, X Wang, Y Wang, Z Zhao, H Zheng, X Ding, *Ind. Eng. Chem. Res.,* 2025, ***64***, 19515-19524.

3 C. Yang, J. Li, C. Yang, Y. Li, A. Hu, J. Pu, B. Chi, *ACS Materials Lett.*, 2024, **6**, 3540-3547.

4 M. Zhang, Y. Chang, W. Xiang, J. Liu, X. Deng, J. Zhou, M. Fu, Z. Tao, *Fuel* 2025,**381**, 133430.

5 S. Oh, I. Jeong, D. Kim, H. Kim, K.M. Roh, K.T. Lee, *Adv. Energy Mater.*, 2025, e03176.

6 F. He, Y. Zhou, T. Hu, Y. Xu, M. Hou, F. Zhu, D. Liu, H. Zhang, K. Xu, M. Liu, Y. Chen, *Adv. Mater.*, 2023, **35**, 2209469.

7 J. Wang, Z. Li, W. Chen, L. Sun, C. Sun, S. Peng, *Small*, 2025, **21**, e09293.

8 X Zhang, C Tang, Y Yang, F Zheng, Q Su, H Xiang, L Meng, L Du, Y Aoki, D Luo, N Wang, S, Ye, *Adv. Funct. Mater.*, 2025, **35**: 2421083.